Investigations on Nano-Soft Composites Exhibiting Liquid Crystalline Phases

A Synopsis of the Thesis to be submitted to the Mangalore University for the award of the degree of Doctor of Philosophy in Physics

Submitted by

Varshini G V

Senior Research Fellow
Registration No- Ref: No.MU/EXB/Ph.D./CR.111/Phy./2019-20/E.13
Enrolment number-178105128
Centre for Nano and Soft Matter Sciences
Bengaluru-562162

Under the supervision of

Dr. D. S. Shankar Rao

Centre for Nano and Soft Matter Sciences (CeNS),
Shivanapura, Bangalore- 562162

Introduction to soft matter:

Soft matter is a young sub field of condensed matter physics. This is a state of matter in which the application of small perturbations will bring out significant changes or responses in the system, whose dynamics are governed by the time scale of seconds. An extensive range of materials which includes emulsions, polymers, colloids, gels, surfactants, emulsions, etc are included in this category. With their complex architecture and anisotropy, these systems are crucial in maintaining our day-to-day lives [1–4]. From an application point of view, advancements in the soft matter field have led to drastic changes in our lifestyles, from witnessing soft robotics to flexible displays. It is also fascinating to know that the biological matters related to DNA, proteins, cell membranes, and related topics also come under soft matter. Studying interactions at the molecular level allows us to recognize their capability significantly from a fundamental perspective. With this brief introduction, we now discuss the topic 'Liquid crystals', a subclass of soft condensed matter, and the main focus of this thesis. The introduction of liquid crystal displays has revolutionized the billion-dollar display industry from TVs to computer screens to trendy smartphones. Besides technological implications, liquid crystal research is very rich from fundamental aspects as well. For example, understanding concepts like critical phenomena, re-entrant phase sequence, elastic deformations, defects and their origin in the microscopic textures, etc. privilege us to realize the nature of microscopic systems [5–11].

Introduction to liquid crystals:

Liquid crystals (LCs) are thermodynamically stable phases of matter observed between the three-dimensionally ordered crystalline solid and the highly disordered isotropic liquid. These states are strongly anisotropic with some of their properties like a crystal and at the same time, exhibiting some properties of a liquid as well. Transition to these states can be brought about either by the effect of temperature or by the influence of solvents. The former is referred to as thermotropic mesomorphism, the latter as lyotropic mesomorphism. Shape anisotropic organic rod like molecules (calamatic), disc-like (discotic), or banana-shaped (bent-core) materials can exhibit liquid crystallinity. These molecules exhibit different phases based on their molecular interactions and arrangement. Thermotropic LC phases exhibited by rod-like molecules are broadly classified into three types: nematic, cholesteric and smectic.

Nematic phase: The nematic (N) is the simplest among all the liquid crystalline phases (see Figure 1(a)). In this phase, the molecules have a long range orientational order but no positional order. The director **n** represents the preferred axis of orientation and is apolar, i.e., + **n** and – **n** are equivalent.

Cholesteric phase: When the molecules exhibiting nematic are optically active, it is called as cholesteric phase (Ch or N*). Ch is essentially a nematic phase, except its structure has a spontaneous twist that is superimposed normal to the director (see Figure 1(d)). The distance over which the director rotates by 360° is called as the pitch of the helix.

Smectic phase: A smectic phase has a stratified (layered) structure in addition to the orientational order. Various smectic phases are possible depending on the type ordering within and between the layers. In the simplest case of the smectic A (SmA) phase, the molecules are upright in each layer, with their centers irregularly spaced in a liquid-like fashion (Figure 1(b)). Smectic C (Sm C) phase is a tilted form of Sm A (see Figure 1(c)).

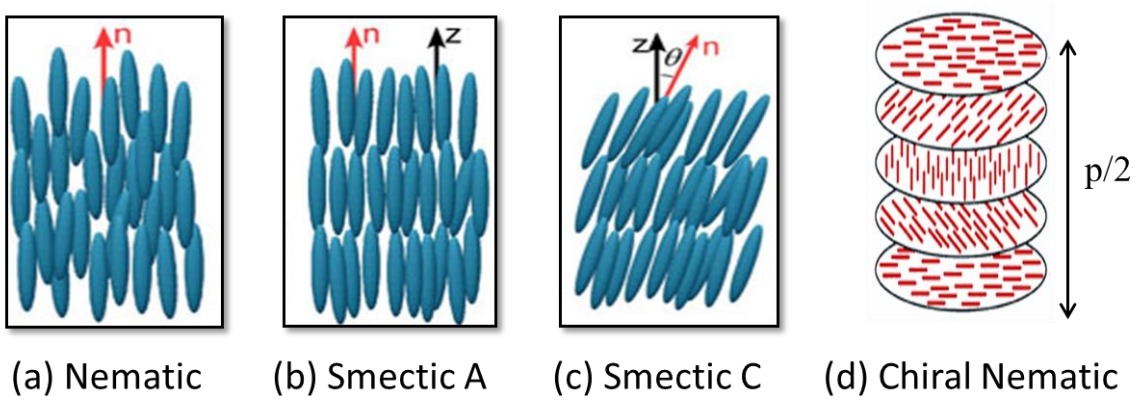

Figure 1: *Schematic representation of molecular arrangement in the (a) Nematic, (b) Smectic A (Sm A), (c) Smectic C (Sm C) and (d) Cholesteric phase.* **n** *represents the director orientation, p- the pitch of the cholesteric helix.*

For a long time, it was believed that only one type of smectic A phase exists, viz., the monolayer SmA_1 phase with the layer spacing d ~ l, the length of the molecule. However, with the synthesis of molecules having a strong polar end group, several types of smectic A phases have been observed, referred to as partially bilayer - SmA_d, (l<d<2l) bilayer - SmA_2 (d~2l) and monolayer - SmA_1 (d ~ l) depending on the extent of interdigitation of the molecules in the neighboring layers. [12,13].

Re-entrant nematic system:

When a compound exhibits nematic and smectic phases, the less ordered nematic phase generally occurs at a higher temperature. As the system is cooled, typically, the higher-ordered phase like SmA is observed. An exception to this rule was discovered by Cladis [14–19] in certain strongly polar materials. The first observation was in a binary mixture of two cyano compounds. Over a range of compositions, the sequence of transition upon cooling was- Iso→N→SmA→Re-entrant nematic (RN) → crystal, which was surprising to observe a less ordered N phase below the SmA.

Bent core Liquid Crystals:

Apart from the rod shape, even the bent-shaped molecules also exhibit liquid crystallinity. Though discovered recently (about two decades ago), bent-core LCs, generally comprising a central rigid core and two linear rigid arms with terminal chains, have attracted much attention, which apart from the usual nematic phase exhibit different mesophases labeled as B1, B2…B8 [20–23].

Twist bend nematic:

Recently, dimers with odd parity hydrocarbon linker between mesogenic arms exhibited another phase called Twist bend nematic (N_{TB}) [24–28]. N_{TB} is similar to the Cholesteric phase but with an essential difference: in the Ch, the helix is orthogonal to the director **n** but it makes an angle (9^o - 30^o) with respect to **n** in the N_{TB} phase (see Figure 2). The pitch of N_{TB} lies in the nanometer range (8-10 nm).

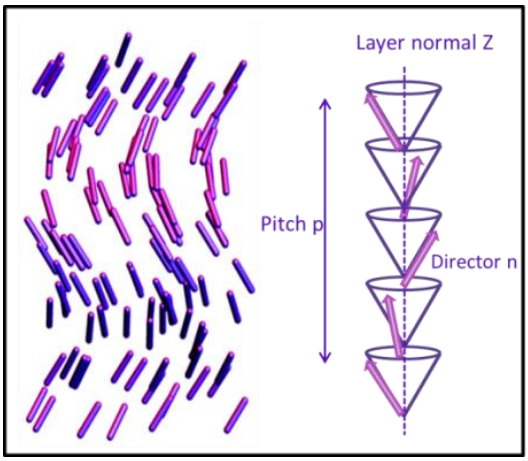

Figure 2: *Schematic representation of molecular arrangement in the twist bend nematic phase.*

Frank elastic constants:

The director may vary spatially due to external fields such as boundary forces, electric or magnetic fields, material flow, temperature gradient, optical or surface effects; this results in elastic deformation, which increases the system's free energy. The deformation energy (F_d) is related to the three principal Frank elastic constants (shown in Figure 3), namely, splay K_{11}, twist $K_{22,}$ and bend K_{33}, and is written as

$$F_d = ½ [K_{11} (\nabla . \vec{n})^2 + K_{22} (\vec{n} . \nabla \times \vec{n})^2 + K_{33} (\vec{n} \times \nabla \times \vec{n})^2]$$

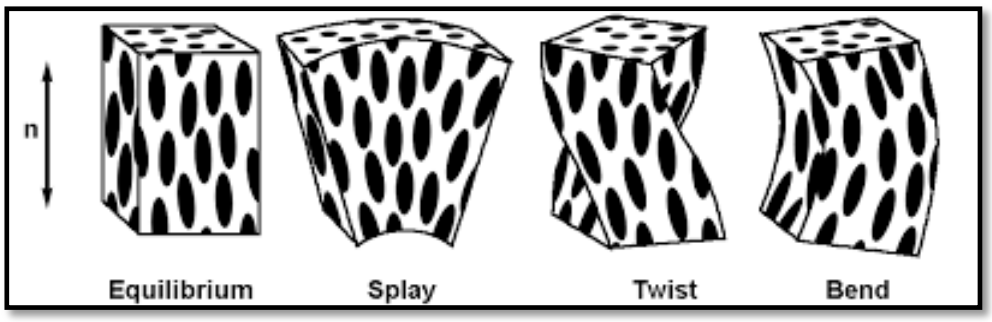

Figure 3: *Schematic diagram showing three principal deformations of the director field in the nematic phase.*

Freedericksz transition:

When the system is under the influence of an external field (magnetic or electric), after a particular threshold value of the field, molecules change their orientation from initial surface driven homeotropic/planar (LC molecules are perpendicular/parallel to the substrate) to the field driven planar/homeotropic alignment, a process defined as field driven Freedericksz transition. This transition is one of the most important electro-optic switching mechanisms for nematic liquid crystals and the foundation for most modern LC Display devices. Freedericksz transition profiles enable the determination of elastic constants.

Organization of the thesis, divided into eight chapters, is as follows:

The introduction to liquid crystals is given in chapter 1. Apart from involving rich fundamental concepts, liquid crystal's remarkable contribution is appreciated in various technological aspects. Whether it is from LCDs to privacy windows or optical waveguides to reflectors or lasers to bio-sensors and so on, it has proven its versatility in various fields. In recent years, many efforts have been put into improving these facets. One of them is obtaining liquid crystalline composites by dispersing several nanoscale structures such as carbon nanotubes, polymer structures, aersoils, gelators etc. There are many attempts to

understand the interplay between the LC molecules and the nanostructures to improvise them from both fundamental and technological perspectives [29–33]. The introduction of anisotropic guest nanostructures in the LC host systems (themselves being anisotropic) affects the phase stability, order parameter, and spatial arrangement of host LCs around the guest materials. Especially when the anisotropy of the guest is much larger than the host LC molecules, the interplay between them leads to quite interesting results.

This thesis deals with such less unexplored areas, shedding light on the LC molecules' unique interactions within themselves and with the guest non LC molecules and nanomaterials. Through such investigations, we have realised that there can be multiple pathways to stabilise or induce a layered smectic phase employing nanoparticles and actinic light explained in chapter 2, chapter 3, and chapter 4. We have demonstrated that single wall carbon nanotube (SWCNT) enhances/induces the SmA_d phase explained in Chapter 2 and 3. Chapter 4 describes the effect of (1) adding non-aromatic polymer (PMMA) in nematic alone and system with reentrant phase sequence, (2) actinic light in systems with double reentrant phase sequence. Chapter 5 showcases studies resulting from the competition between - soft bent and rigid bent cores system having twist bend nematic phase. Chapters 6 and 7 deals with the study on the influence of sample thickness, pressure, and confinement effect on the formation of gel networks. Chapter 7 describes the summary of all the chapters and the outlook of the thesis.

Chapter 1: Introduction to liquid crystals

This chapter describes the introduction to liquid crystals, classification, the associated concepts and the scope of the thesis.

Chapter 2: Suppression of the re-entrant nematic and stabilization of the smectic phases by carbon nanotubes

This chapter describes the influence of single wall carbon nanotube (CNT) doping in a host LC (HLC) system that has the re-entrant (N-SmA_d-RN) phase sequence. Despite the fact that both components are rod-like anisotropic structures, the presence of CNT, even though in the dilute concentration limit, significantly influences the thermal behaviour of the host LC

system. The smectic A thermal range gets enhanced (more than double when compared with host LC) at the expense of nematic and RN phase temperature range as shown in Figure 4.

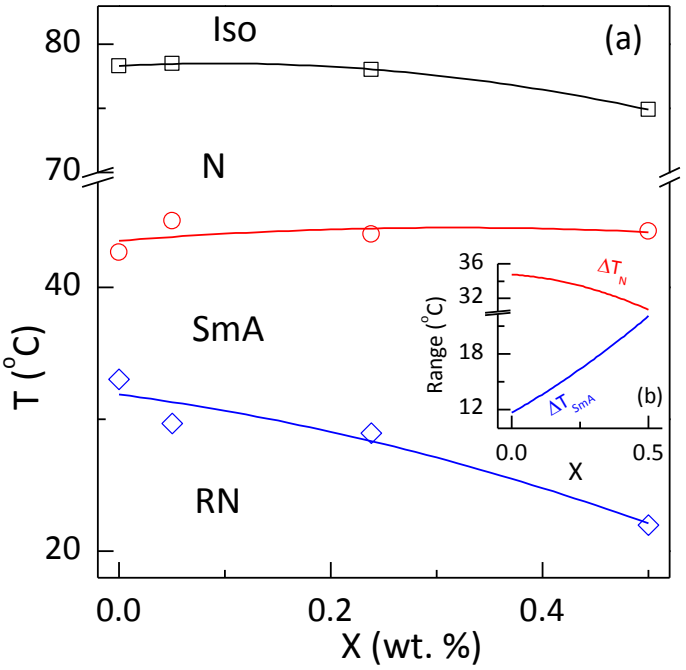

Figure 4: *(a) Temperature-concentration phase diagram of HLC/CNT with X being the weight % of CNT. The Iso-N and the* SmA_d *-RN transition temperatures diminish with an increase in X, the latter having a larger change; the thermal range of the nematic phase (*ΔT_N*) decreases slightly, that of the smectic phase (*ΔT_{SmA}*) increases drastically as depicted in the inset (b), occurring at the expense of the N and RN phase temperature range.*

The magnetic field driven Freedericksz transformation measurements show higher enhancement for the splay deformation (K_{11}) than the bend deformation (K_{33}) which is due to the higher aspect ratio (~250) of the CNT as compared to that for the host LC molecules (~5).

Both HLC and the composites exhibit significant short-range smectic order in the N and RN phases. Dielectric measurements indicate the inherent favour towards antiparallel correlation between neighbouring liquid crystal molecules, which further gets increased when CNTs are present. Supporting this behaviour, X-ray diffraction measurements also reveal a better antiparallel correlation for the HLC+CNT composite. The magnetic field-changeable electrical conductivity of the medium is proposed as a possible conductivity switch. We propose a molecular model based on a combination of Flory Huggins and Landau's theory for the stabilization of the smectic phase upon the introduction of CNT.

Chapter 3: Nanophase Segregation of Nanostructures: Induction of Smectic A and Re-Entrance in a Carbon Nanotube/Nematic Liquid Crystal Composite

This chapter demonstrates the effect of SWCNT in a similar host system as discussed in the previous chapter but with the difference in the host LC exhibiting only a nematic phase. Upon doping small amounts of CNT into the 'only nematic' host LC, the smectic phase gets induced along with the presence of a re-entrant nematic phase at low temperature. Proof for the appearance of the smectic phase is provided through optical microscopy, Frank elastic constant (Figure 5 (a)), laser transmission (Figure 5 (b)), and X-ray diffraction (XRD) studies.

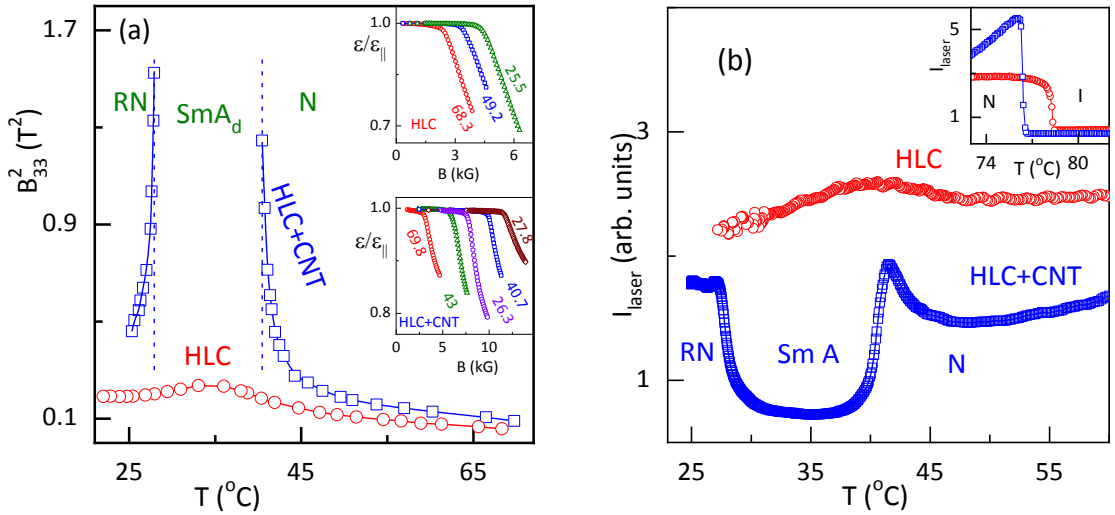

Figure 5: *Thermal variation of (a) The threshold B_{33}^2 and (b) transmitted laser intensity (I_{laser}). The HLC presents a weak thermal dependence for both B_{33}^2 and I_{laser} as shown in (a) and (b). The composite shows (a) critical divergence for B_{33}^2 on approaching the smectic phase from both N and RN phases, whereas in (b) exhibits abrupt changes in I_{laser} which correspond to the N-SmA$_d$ and SmA$_d$ -RN transitions. The insets in (a) show the raw profiles of the Freedericksz transition, (b) shows the changes seen across the isotropic-nematic transition, which is lower by about 1.8 °C for the composite.*

Below the isotropic point the HLC shows only the N phase right down to room temperature with a characteristic mosaic texture. In contrast, the HLC + CNT composite shows a richer behaviour: cooling from the isotropic phase the sample exhibits a mosaic texture first, but at a lower temperature transforms to a fan-shaped texture that signifies the presence of the SmA$_d$ phase. Further cooling results in the return of the mosaic texture obtaining the phase sequence of N– SmA$_d$–RN with the induction of the SmA$_d$ phase. The critical field B_{33} which indicates

deviation from the initial surface-dictated homeotropic to magnetic field driven planar orientation, directly measures the bend elastic constant (K_{33}). B_{33} shows weak temperature dependence for HLC but large non-monotonic variations for the composite characteristic of the N−SmA_d transition (Figure 5 (b)). A mirror-like behavior below 28 °C, as expected for the SmA_d−RN transition is seen at a lower temperature. The observation of induced smectic A_d and the resultant re-entrant phase sequence (N-SmA_d-RN) are supported by the XRD study, Raman spectroscopic measurements

Chapter 4: Appealing pathways to stabilize/induce an ordered phase in a system exhibiting a reentrant sequence

We discussed the induction/stabilization of the smectic A phase by adding rigid anisotropic CNTs to the host liquid crystal. In addition to CNT, this chapter discusses other pathways to stabilise the smectic phase with two subsections (a) non-aromatic polymer and (b) photo-isomerizable compound.

In fact the presence of these components favours the SmA_d phase at the expense of the re-entrant nematic phase (RN). Figure 6 represents the POM images at selected temperatures for the host LC and its composite with PMMA. While the former shows, at all temperatures, the characteristic mosaic texture of the N phase, the composite shows the mosaic texture at higher and lower temperatures and the chevron and polygonal textures at intermediate temperatures, establishing the fact that the SmA_d phase is induced with the consequent appearance of the reentrant phase sequence.

The second part of the chapter discusses the anomalous photoinduced shift in a material with multiple re-entrant phases, viz., N-SmA_d-RN-SmA_{re}, with the high temperature SmA_d and the SmA_{re} phases having partially bilayer and monolayer characteristics, respectively. The material is photo-active with an azo linkage group in the structure and is a polar molecule. Figures 7 (a) and (b) present the thermal variation of the laser transmission (I_T) for no UV and with-UV conditions. The UV radiation has the strongest influence on the RN-SmA_1 transition; it is least on the N-SmA_d with SmA_d-RN having the intermediate effect. Secondly, the diminution in the RN-SmA_1 and SmA_d-RN transition temperatures with I_{UV} is non-monotonic.

For example, in the case of RN-SmA_1 transition, δT, the photoinduced shift in the corresponding transition temperature, is more for 0.5 mW/ cm^2 than for 15 mW/cm^2. Some

of the features are well explained with the combination of the nanophase segregation mechanism and the frustrated spin gas model, whereas the puzzling photo-driven behaviour of the re-entrant nematic and re-entrant smectic lines needs more elaborate understanding [34–36].

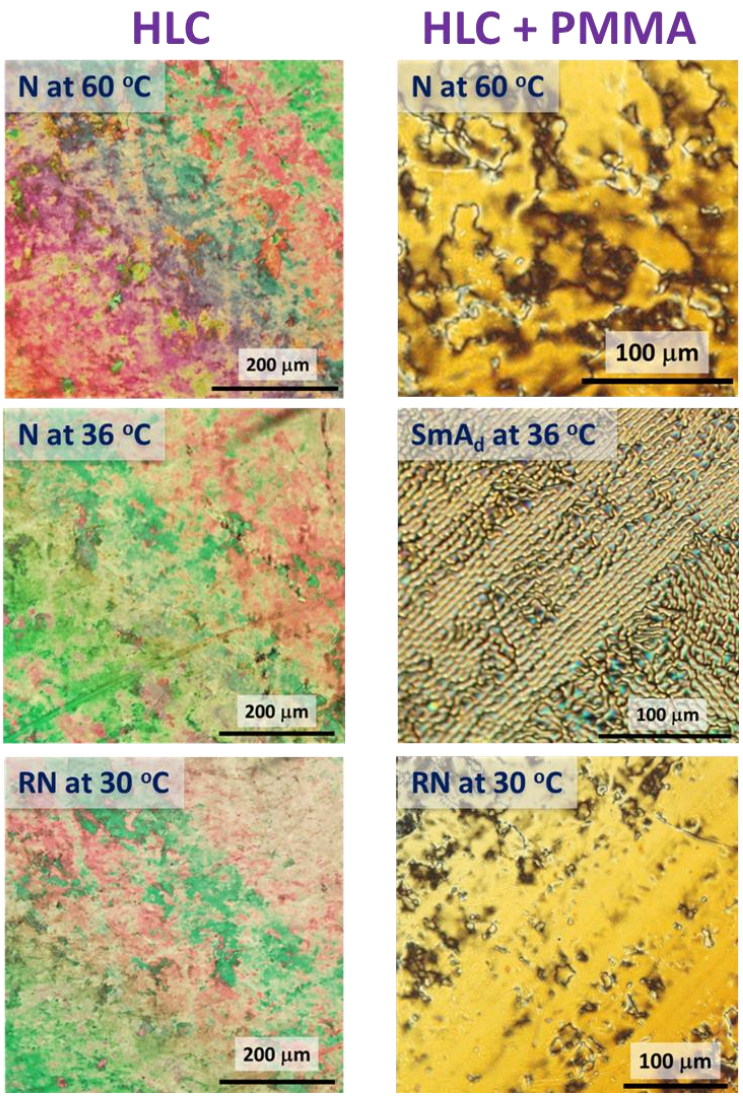

Figure 6: *POM images for without (left panel) and with PMMA (right panel). Images with PMMA show the induction of the SmA_d phase and the consequent appearance of the reentrant phase sequence, whereas the material without PMMA exhibits the nematic mesophase only.*

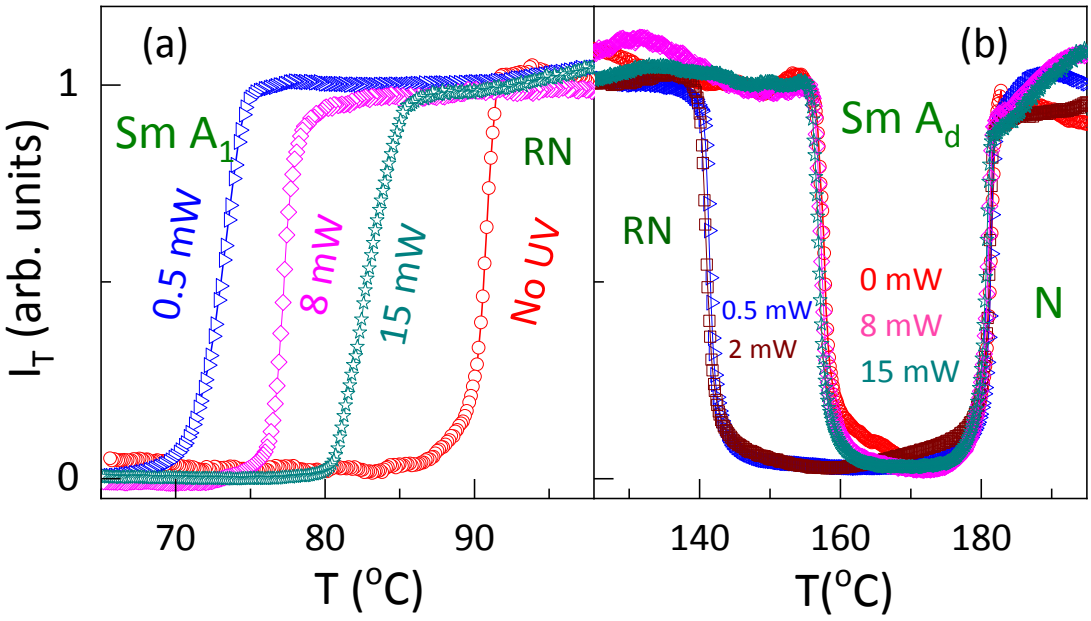

Figure 7: *Temperature versus I_T profiles across (a) RN-SmA_1 and (b) N-SmA_d-RN sequence transition for different UV intensities. The photo-driven shift in the transition temperature is minimum for N-SmA_d, maximum for RN -SmA_1, and intermediate for SmA_d -RN transition.*

Chapter 5: Dielectric and viscoelastic investigations in a binary system of soft- and rigid-bent mesogens exhibiting the twist-bend nematic phase

One of the important findings in recent years is the discovery of the twist bend nematic (N_{TB}) phase that differs from the typical nematic or its chiral counterpart, the chiral nematic (cholesteric, Ch). In this phase, the helix axis makes an angle (between 9^o - 30^o) with the director unlike in the cholesteric phase where the helix is orthogonal to the director. N_{TB} phase is generally observed in a flexible dimer with an odd spacer linkage. This chapter investigates a binary system wherein both the constituents have bent shapes but vary in rigidity in their bent structure. The propensity of bent architecture towards the twist-bend structures is evident because the N_{TB} phase gets induced by adding even a small amount of the soft-bent material and exists over an extensive range of concentration (Figure 8). The investigated dielectric and viscoelastic behaviour provides rich information on subtle alterations in the molecule's central bend portion and substantially influences physical properties.

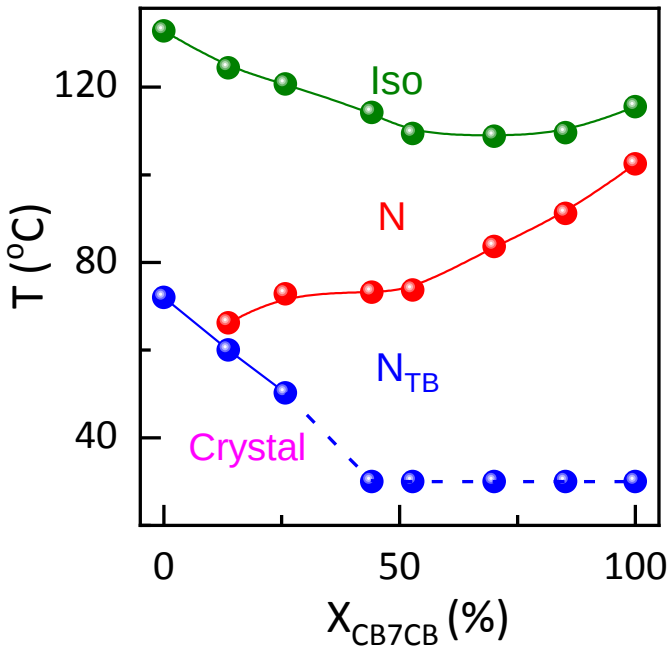

Figure 8: *Temperature-concentration phase diagram of soft dimer in rigid bent dimer with X_{CB7CB} indicating the concentration of soft dimer. With increasing X_{CB7CB}, the transition temperatures of the Iso-N and N-N_{TB} boundaries move in opposite directions, diminishing the thermal range of the nematic phase.*

Permittivity data in the isotropic phase reveal that antiparallel correlation becomes strongest for an intermediate concentration suggesting better coupling of the extended conformers of both soft and rigid bent core materials. Dielectric spectroscopy measurements reveal that two modes are present, attributed to the fluctuations of clusters (group of molecules and thus much heavier than individual molecules) and the rotation of individual molecules around their short axes over a wide span of compositions in this binary system. Besides exhibiting the expected feature of the bend elastic constant (K_{33}) being lower than its splay constant (K_{11}), the elastic constant measurements also throw light on the possibility of obtaining an elastic isotropic point ($K_{33} = K_{11}$) in such binary systems. The rotational viscosity is also twin-valued with the lower viscosity γ_{11} being more weakly dependent on temperature than the higher viscosity γ_{12}. These two values are ascribed to the cluster and individual modes as mentioned earlier. These observations are explained through multiple conformations of the two types of molecules, namely extended and horseshoe type of soft dimer and only extended conformer for a rigid bent molecule.

Chapter 6: Anisotropic sol-gel transition: Influence of sample thickness and applied pressure, and rheological behavior

Introducing confinement has been proven to enhance the morphological, optical, and dielectric properties of liquid crystals [37]. The contents of the chapter are divided into two parts. The first part mainly focuses on the effect of sample thickness and applied pressure on the gelation temperature. For the present study, a gelator is added to a nematic host which exhibits nematic sol to nematic gel transition. In a study first of its kind, we have observed that there is a significant effect of sample thickness on the gelation temperature. The nematic sol-nematic gel transition temperature increases with increase in the thickness of the sample and reaches a plateau of around > 30 μm as shown in Figure 9. Rheological studies have also been carried out to study the storage and loss modulus of these systems. While strain dependence of storage and loss moduli exhibit the Payne effect/weak strain overshoot, the magnitudes of the moduli and their thermal variation present explicit dependence on d, both behaviours being well described by power-law expressions. Studies at elevated pressures also corroborate the observations of d-dependence with the nematic sol thermal range increasing with P, suggesting reduced favour for network formation.

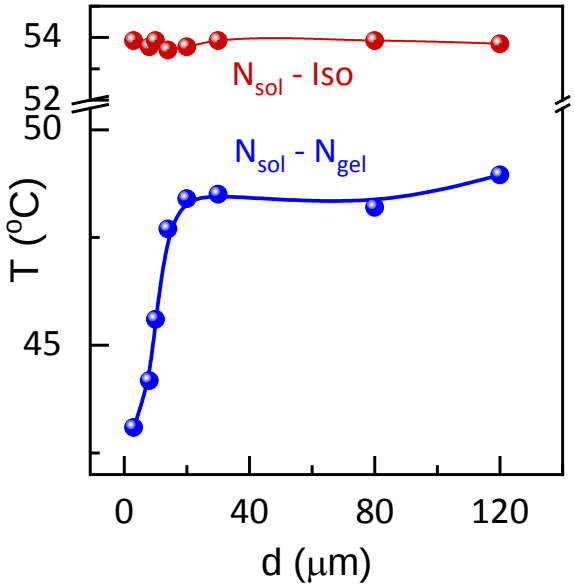

Figure 9: *The variation of $T_{N\text{-}Iso}$ and $T_{Nsol\text{-}Ngel}$ temperatures vs. sample thickness. It is observed that the Iso-N transition temperature shows minor/no changes with sample thickness, whereas the gelation temperature drops significantly for thinner samples and saturates after ~ 30μm.*

Chapter 7: Morphological aspects of a hierarchical network of nematic gel and a superimposed photopolymer

Polymer stabilized liquid crystals (PSLCs) are a class of materials that are quite famous for various application like electrically controlled smart windows. Observing the influence of sample thickness on gelation in the previous chapter, we present here the studies on hierarchical network formation in an anisotropic environment and comprehend its impact on the gelation and also on the morphology of the formed network. In fact, these types of double networks with different materials have enormous potential in drug delivery systems, tissue engineering, biosensors, and so on [38–41]. Using a photo-polymerisable monomer RM82, the second network is made to form in the host LCG. Detailed studies have been conducted to investigate the mutual influence of these networks formed on the morphology and the gelation properties of the LCG. Experiments have been carried out with varied (1) monomer concentrations and (2) temperature at which the sample is polymerized. Polymerizing the sample in different phases has enabled us to study the effect of LC orientations on the network formation which can be observed in POM images shown in Figure 10 along with the varied concentration of photopolymer as well. Polymerizing in the isotropic phase does not aid the formation of strands. But polymerization carried out in the nematic and gel phase of the host LCG exhibits droplet morphology for low polymer concentration, but better strands are formed with an increase in polymer concentration. Well oriented dense strands are seen for higher polymer concentration in both gel and nematic polymerized samples. Morphological studies have been carried out through SEM images which showcase the alignment of strands at a microscopic level. Through SEM images, porosity and fractal dimension have also been calculated, which reveals that the nematic polymerized sample has higher porosity than the gel polymerized sample. Fractal dimension is also seen to be higher for the nematic polymerized than the gel polymerized sample. A phase diagram is constructed between the gelation temperature and RM82 concentration with polymerisation carried out in three different phases. It has been observed that the effect on gelation temperature is highly non-monotonic for intermediate RM82 and the highest impact is seen in the case of a nematic polymerised sample. The above observations are explained considering the factors like the temperature at which the polymerization was carried out, monomer concentration in the system, and mutual influence of the networks existing.

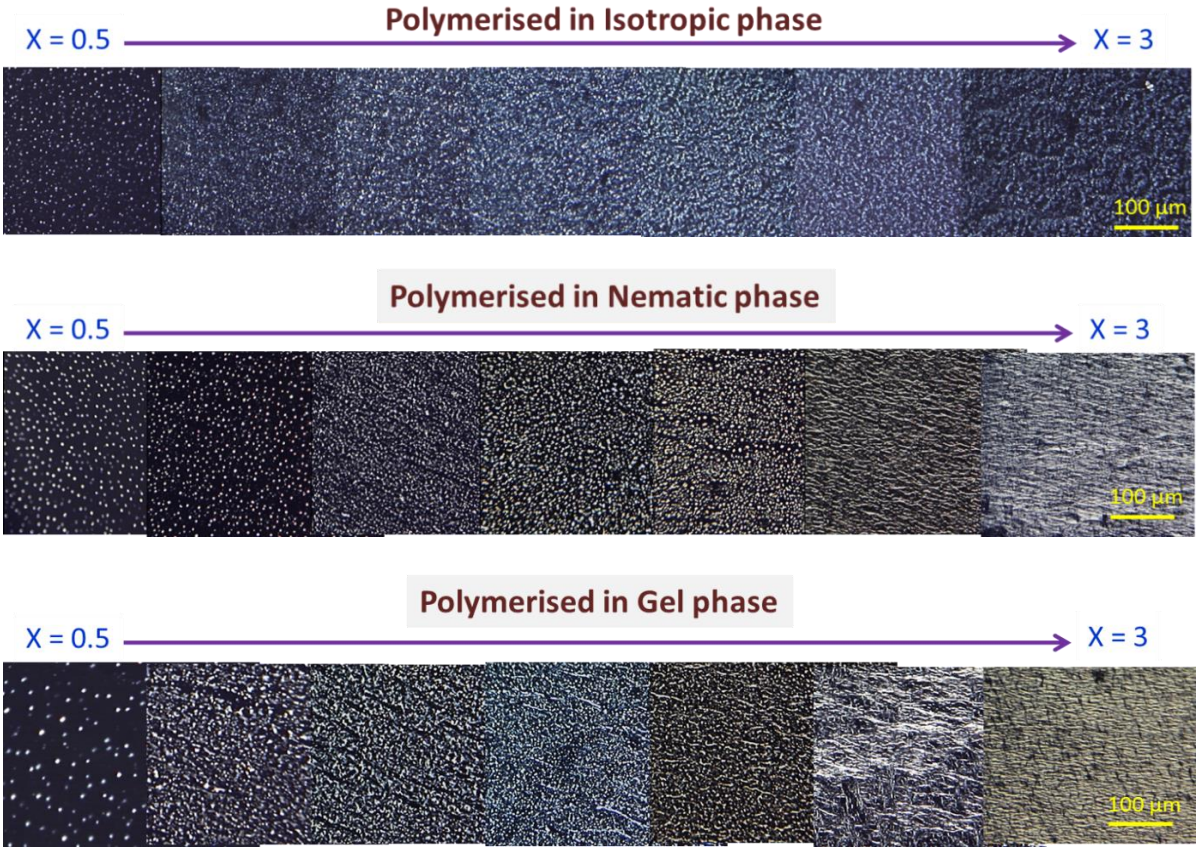

Figure 10: *POM images taken in the isotropic for different polymerising conditions with varied RM82 concentrations from X = 0.5 to 3 wt % of RM82 in host LCG. Strand formation can be better observed for nematic and gel polymerised samples compared to isotropic polymerized samples.*

Chapter 8: Summary and outlook

This chapter provides a comprehensive overview of the work described in chapters 2-7 and a future outlook.

References

1. P. G. De Gennes, Rev. Mod. Phys. **64**, 645 (1992).

2. P. G. De Gennes, Soft Matter **1**, 16 (2005).

3. Richard A.L. Jones, *Soft Condensed Matter* (Oxford University Press, New York, 2002).

4. M. Kleman and O.D Lavrentovich, in (Springer-Verlag, New York Inc, 2003).

5. S. Chandrasekhar, *Liquid Crystals*, 2nd ed. (Cambridge University Press, 1994).

6. P. J. Collings and M. Hird, *Introduction to Liquid Crystals* (CRC Press, 1997).

7. D. Demus, J. Goodby, G. W. Gray and H. W. Spiess, *Handbook of Liquid Crystals* (Wiley-VCH, 1998).

8. Robert H. Chen, *Liquid Crystal Displays, Fundamentals Physics and Technology* (Wiley and Sons, 2011).

9. P. G. de G. Prost, J, *The Physics of Liquid Crystals* (Oxford Science Publication, 1993).

10. S. T. W. D.K. Yang, *Fundamentals of Liquid Crystal Devices* (John Wiley & Sons Ltd, England, 2015).

11. B. Bahadur, *Liquid Crystals Applications and Uses* (World Scientific Publishing Co. Pte Ltd, 1992).

12. J. Prost, Adv. Phys. **33**, 1 (2006).

13. M. F. A. and G. S. F. Hardouin, A. M. Levelut, J. Chim. Phys. **80**, 53 (1983).

14. P. E. Cladis, Phys. Rev. Lett. **35**, 48 (1975).

15. P. E. Cladis, R. K. Bogardus, W. B. Daniels, and G. N. Taylor, Phys. Rev. Lett. **39**, 720 (1977).

16. N. V. Madhusudana, K. L. Savithramma, and S. Chandrasekhar, Pramana **8**, 22 (1977).

17. N. V. Madhusudana and S. Chandrasekhar, Pramana Suppl. **1**, 57 (1973).

18. A. J. Leadbetter, R. M. Richardson, and C. N. Colling, Le J. Phys. Colloq. **36**, C1 (1975).

19. A. Leadbetter, J. Frost, J. Gaughan, G. Gray, A. Mosley, A. J. Leadbetter J C Frost J P Gaughan, and G. W. Gray, J. Phys. **40**, 375 (1979).

20. T. Niori, T. Sekine, J. Watanabe, T. Furukawa, and H. Takezoe, J. Mater. Chem. **6**, 1231 (1996).

21. K. E. Vorlander D, Fuchs K, Ber Dtsch Chem Ges. **62**, 2381 (1929).

22. D. R. Link, G. Natale, R. Shao, J. E. Maclennan, N. A. Clark, E. Körblova, and D. M. Walba, Science **278**, 1924 (1997).

23. M. Hird, Liq. Cryst. Today **14**, 9 (2005).

24. V. P. Panov, M. Nagaraj, J. K. Vij, Y. P. Panarin, A. Kohlmeier, M. G. Tamba, R. A. Lewis, and G. H. Mehl, Phys. Rev. Lett. **105**, 167801 (2010).

25. I. Dozov, Europhys. Lett. **56**, 247 (2001).

26. P. A. Henderson and C. T. Imrie, Liq. Cryst. **38**, 1407 (2011).

27. M. Cestari, E. Frezza, A. Ferrarini, and G. R. Luckhurst, J. Mater. Chem. **21**, 12303 (2011).

28. C. Meyer, G. R. Luckhurst, and I. Dozov, J. Mater. Chem. C **3**, 318 (2014).

29. Quan Li, *Nanoscience with Liquid Crystals* (Springer, 2014).

30. J. P. F. Lagerwall and G. Scalia, *Liquid Crystals with Nano and Microparticles* (World Scientific Publishing Co. Pte Ltd, 2016).

31. S. P. Yadav and S. Singh, Prog. Mater. Sci. **80**, 38 (2016).

32. C. Zakri, Liq. Cryst. Today **16**, 1 (2007).

33. J. P. F. Lagerwall and G. Scalia, **18**, 2857 (2008).

34. C. A. Guymon, E. N. Hoggan, N. A. Clark, T. P. Rieker, D. M. Walba, and C. N. Bowman, Science (80-.). **275**, 57 (1997).

35. Y. Lansac, M. A. Glaser, N. A. Clark, and O. D. Lavrentovich, Nature **398**, 54 (1999).

36. S. K. Prasad, G. G. Nair, and G. Hegde, Adv. Mater. **17**, 2086 (2005).

37. S. Krishna Prasad, M. Baral, A. Murali, and S. N. Jaisankar, ACS Appl. Mater. Interfaces **9**, 26622 (2017).

38. U. Farooq, J. Teuwen, and C. Dransfeld, Polym. 2020, Vol. 12, Page 1908 **12**, 1908 (2020).

39. S. Ishikawa, K. Iijima, D. Matsukuma, Y. Asawa, K. Hoshi, S. Osawa, and H. Otsuka, Chem. Mater. **32**, 2353 (2020).

40. J. P. Gong, Y. Katsuyama, T. Kurokawa, and Y. Osada, Adv. Mater. **15**, 1155 (2003).

41. A. S. Krishnan, P. H. Vargantwar, and R. J. Spontak, Undefined **8**, 12025 (2012).

List of publications and book chapter

The following is the list of publications and book chapter resulting from the work carried out by the candidate:

1. **G. V. Varshini**, D. S. Shankar Rao, P. K. Mukherjee, and S. Krishna Prasad, "Nanophase Segregation of Nanostructures: Induction of Smectic A and Re-Entrance in a Carbon Nanotube/Nematic Liquid Crystal Composite."
   J. Phys. Chem. B. **122 (47)**, 10774 (2018).

2 **G. V. Varshini**, D. S. Shankar Rao, P. K. Mukherjee, and S. Krishna Prasad, "Suppression of the re-entrant nematic and stabilization of the smectic phases by carbon nanotubes."
   J Mol. Liq. **286**, 110858 (2019).

3. **G. V. Varshini**, D. S. Shankar Rao, U. S. Hiremath, C. V. Yelamaggad and S. Krishna Prasad, "Dielectric and viscoelastic investigations in a binary system of soft- and rigid-bent mesogens exhibiting the twist-bend nematic phase."
   J Mol. Liq. **323**, 114987 (2021).

4. **G. V. Varshini**, Pragnya Satapathy, D. S. Shankar Rao, S. Krishna Prasad, "Multiple pathways to stabilize/induce an ordered phase in a system exhibiting a re-entrant sequence."
   Liq. Cryst. **49**, 952 (2022) (Invited article).

5. **G. V. Varshini,** P. Srividhya, D.S. Shankar Rao, S. Krishna Prasad, "Anisotropic sol-gel transition: Influence of sample thickness and applied pressure, and rheological behaviour"; Manuscript communicated, under review.

6. **G. V. Varshini**, D. S. Shankar Rao, S. Krishna Prasad; "Morphological aspects of a hierarchical network of nematic gel and a superimposed photopolymer."
   Manuscript under preparation.

*A **book chapter** has a partial contribution from the research work presented in this thesis-*

"Influence of Gulliver over Lilliput: Novel Properties of Carbon Nanotube/Liquid Crystal Composites", S. Krishna Prasad, D.S. Shankar Rao, Marlin Baral, **G. V. Varshini**, Chapter 3, 23 pages, Organized Networks of Carbon Nanotubes, Taylor & Francis Group, New York 2020.

Publications from the collaborative works but not included in the thesis:

7. Subir Roy, I. Sivakumar, F. Francis, **G. V. Varshini** and S. Angappane, "Observation of Room-Temperature Low-Field Magnetoresistance in Reduced Graphene Oxide/ $CoFe_2O_4$Nanocomposites."
   Phys. Status Solidi B, **258**, 2100033, (2021).
8. Subir Roy, H.R. Nikhita, **G. V. Varshini**, A.K. Patra, R.B Gangineni and S. Angappane, "Enhancement of Room-Temperature Magnetoresistance in Polyvinyl Acetate Encapsulated Fe_3O_4 nanoparticles."
   J. Magn. Magn. Mater., **557**, 169468, (2022)